

Application of lock-in thermography non destructive technique to CFC armoured plasma facing components

F. Escourbiac ^{*}, S. Constans, X. Courtois, A. Durocher

Association Euratom-CEA, CEA/DSM/DRFC, CEA/Cadarache, F-13108 Saint Paul Lez Durance, France

Abstract

A non destructive testing technique – so called modulated photothermal thermography or lock-in thermography – has been set-up for plasma facing components examination. Reliable measurements of phase contrast were obtained on 8 mm carbon fiber composite (CFC) armoured W7-X divertor component with calibrated flaws. A 3D finite element analysis allowed the correlation of the measured phase contrast and showed that a 4 mm strip flaw can be detected at the CFC/copper interface.

© 2007 Elsevier B.V. All rights reserved.

1. Introduction

Plasma facing components (PFC) commissioning is a key issue for actively cooled fusion machines [1]. In particular, the thermal behaviour of the commissioned PFC must be assessed in order to guarantee the integrity of the multilayer components during its lifetime. Previous studies [2] indicates that, due to the technological complexity of actively cooled PFC, it is necessary to cross-check different NDT techniques. Therefore, a modulated photothermal thermography or lock-in thermography technique recently has been set-up in CEA/DRFC. This technique currently used in nuclear fusion [3] and in the aerospace industry [4], is based on the study of ther-

mal wave propagation into the examined sample produced by an external sinusoidal thermal stimulation as depicted in Fig. 1. The thermal response of the component is recorded during the stimulation with an infrared device. Dedicated software and a synchronisation device perform the Fourier analysis at each pixel of the IR image. The calculated phase-shift depends on the thermal diffusivity along the heat path so that the presence of flaws into the component, in particular in-between the multilayer interfaces can be detected.

No mechanical contact, no physical coupling nor cooling are required for this technique. Furthermore, the phase-shift is not dependent on optical properties of the sample or on the heat flux deposition pattern, usual difficulties in thermography. The lock-in technique was operated on carbon fibre composite armoured PFC. This paper deals with the experimental protocol and modelling performed to estimate quantitatively the flaws that can be detected at the CFC/copper interface.

^{*} Corresponding author. Address: Département de Recherches sur la fusion Contrôlée, DRFC/SIPP, Bât. 506, CEA/Cadarache, F-13108, Saint Paul Lez Durance cedex, France. Tel.: +33 0 442 25 44 00; fax: +33 0 442 25 49 90.

E-mail address: frederic.escourbiac@cea.fr (F. Escourbiac).

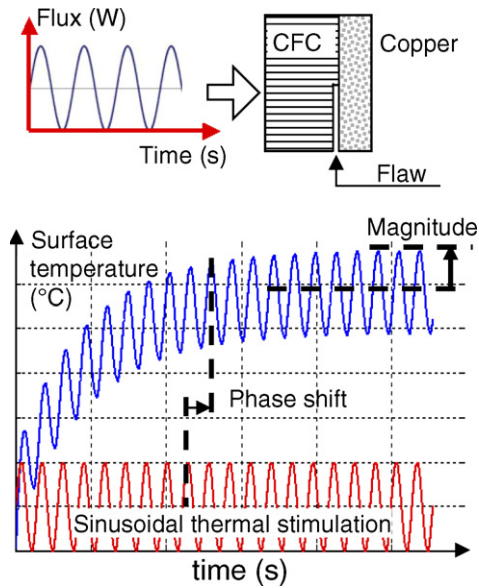


Fig. 1. Principle of thermal wave propagation into a thermally stimulated component.

1.1. Test bed

The test set-up is shown in Fig. 2. It includes an infrared camera (range 3–5 μm, 320 * 240 pixels/frame, 50 Hz sampling rate), a set of 8 halogen lamps (8 × 1 kW electrical power), a function generator providing the reference signal, a power regulator, a synchronisation device (also called lock-in box) which synchronises the IR frames with the reference and a computer. The ALTAIR-LI software (CEDIP Company) monitors the camera and the lock-in box, calculates the demodulation for each

pixel of the IR frames, stores and displays the cartographies of phase-shift and the front face temperature video.

1.2. Examined PFC

The first set of experiments to refine the technique was performed on a CFC tile (trademark Sepcarb® NB31) joined to oxygen free high conductivity (OFHC) Copper (22 mm × 19 mm, CFC and copper thicknesses, respectively, 6 and 2 mm) by a direct joining process developed by Politecnico de Torino [5]. X-ray micro tomography examination of this PFC did not indicate the presence of any

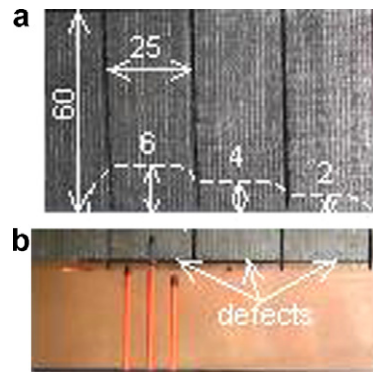


Fig. 3. W7-X divertor PFC with artificial calibrated defects (dimensions in mm). (a) Front view of the component (zoom on 4 tiles) with indication by transparency of 6, 4 and 2 mm width defects machined in-between CFC NB31 and copper layer. (b) Lateral view of the component with the horizontal 0.3 mm thickness traces of the tool (the 3 vertical parallel grooves are for thermocouple implementation).

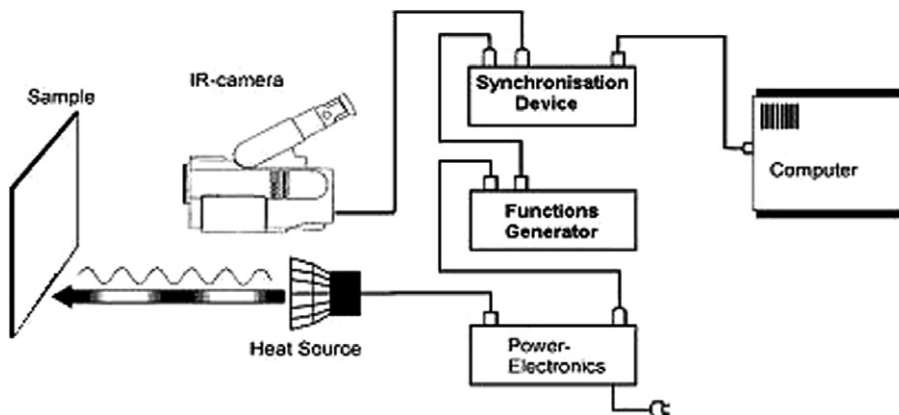


Fig. 2. Lock-in thermography test bed.

flaws. The second set of experiments for protocol validation was performed on a stellerator WENDELSTEIN 7-X (W7-X) divertor PFC composed of CFC NB31 tiles assembled by Plansee AMC® process to a OFHC copper layer (60 mm width × 25 mm length, CFC and pure copper thicknesses, respectively, 8 and 3 mm) then electron beam welded onto a CuCrZr heat sink [6]. This dedicated PFC was manufactured with artificial flaws on the edge of the CFC/copper interface of 3 tiles. Each edge defect was machined on the full length of the tile, with a different width for each tile, respectively, 2, 4 and 6 mm as shown in Fig. 3.

2. Modelling

2.1. Estimation of the stimulation frequency

In an isotropic and homogeneous medium, the thermal wavelength Λ of a sinusoidal stimulation is given by $\Lambda = \sqrt{4\pi a/f}$ (a being the diffusivity of the stimulated material and f the stimulation frequency). For a depth defined as the skin thickness $\mu = \Lambda/2\pi$, the magnitude of the thermal signal is 37% of the surface magnitude. When the skin thickness is one third of the wall thickness, i.e., when the frequency is higher than $f_{lim} \approx 9a/\pi e^2$, the thermal wave does not propagate to the backside and the medium behaves as if it were semi-infinite. In our application, for 6–8 mm of CFC NB31 ($a = 230 \cdot 10^{-6} \text{ m}^2/\text{s}$), $f_{lim} \sim 10 \text{ Hz}$.

To better estimate the most efficient stimulation frequency taking account of the presence of a flaw, a theoretical 1D model solving the steady-state heat conduction problems in a multi-layer isotropic and homogeneous wall under periodic heating was written by using the thermal quadrupole methods and inverse Laplace transform [7]. One benefit of this model is that a flaw between two layers can be easily represented by an air layer ($a = 22 \cdot 10^{-6} \text{ m}^2/\text{s}$). The front surface temperature phase-shift versus frequency was calculated with an air thickness layer as a parameter. The limit frequency of 10 Hz was confirmed (phase shifting of 45° represents semi-infinite wall behaviour) and the best *phase contrast* (difference of phase-shift between a sample with flaw and a sample without flaw) was found in the stimulation frequency range of 0.1–1 Hz (Fig. 4). However, *phase contrast* and stimulation frequency evaluated with this simple linear model must be considered as an indication only; experimental assessments are necessary.

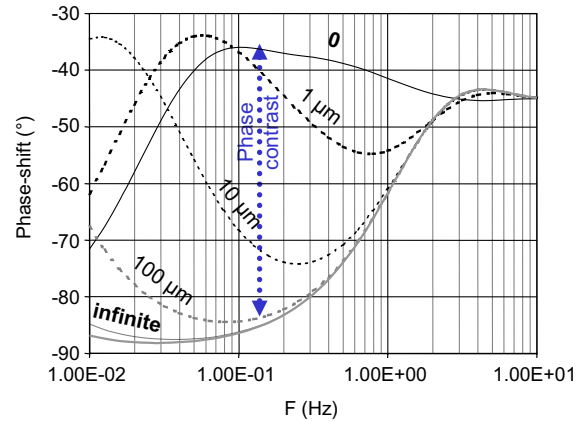


Fig. 4. Front surface temperature phase-shift versus frequency calculated with air thickness layer as a parameter.

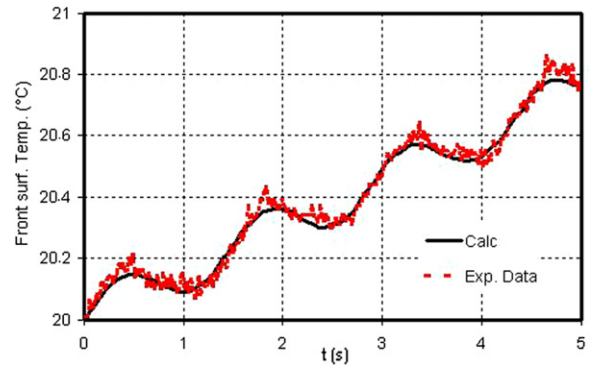


Fig. 5. Front surface temperature of sample without flaw compared with 3D modelling – $F = 0.7 \text{ Hz}$ – this corresponds to a sinusoidal absorbed heat flux of 4 kW/m^2 .

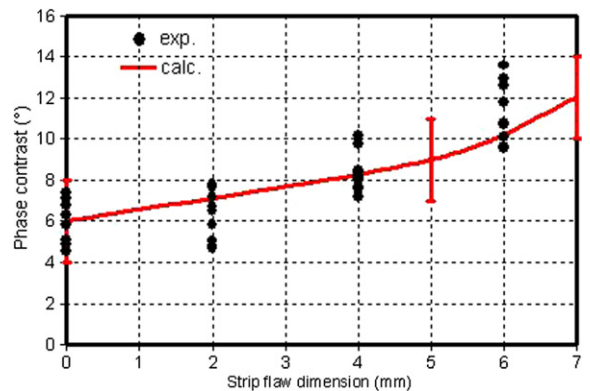


Fig. 6. Comparison between experimental (symbols) and calculated (line with error bar) phase contrast on W7-X divertor PFC with artificial calibrated defects.

2.2. Finite element analysis

A 3D model solving the heat conduction problems in a multi-layer homogeneous wall under periodic heating was built with ANSYS Finite Element software. It included anisotropy of CFC NB31, radiative transfer, a convective boundary condition and the presence of a flaw modelled as the presence of air in-between CFC NB31 and copper layers. Transient calculations allowed an estimation of the incident heat flux from the lamps (Fig. 5), afterwards, steady-state calculations were successfully compared with experimental results (Fig. 6).

3. Experimental results and discussion

Examination of the component without a flaw was performed at 0.1–1 Hz (by looking visually for a best image contrast and signal/noise ratio). The phase-shift was computed by pixel and represented as a cartography. The experimental absolute value of the phase-shift was not reproducible. Conversely, the *phase contrast*, the relative value defined as the difference between maximum and minimum phase-shift on a cartography, appears to be a reliable measurement if the following experimental parameters are taken into account:

- Number of periods for demodulation calculation (the signal/noise ratio increases with the square root of the number of periods): phase contrast was repetitively measured from the same infrared video, increasing the number of periods up to stabilization, typically after ~30 periods as depicted in Fig. 7;

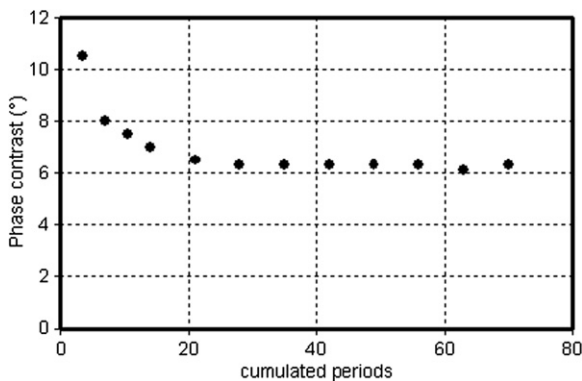


Fig. 7. Phase contrast evaluation vs cumulated period for demodulation (exp. parameters: $f = 0.7$ Hz, quasi steady-state, $n = 9$).

- Thermal regime: Thirty-four examinations were performed of the same component, phase-shift cartographies were measured arbitrarily during transient and quasi steady-state regime. The corresponding phase contrasts were plotted versus derivative of average temperature $\bar{T}(t)$ with respect to time ($\bar{T}(t)$ being defined by $T(t) = \bar{T}(t) + \delta T(t)$ where $T(t)$ is the measured front face temperature and $\delta T(t)$ the sinusoidal fluctuation). A large scattering of measured phase contrasts was found for transient regime but tended to a stabilized value in the steady-state regime, typically for $DT/dt < 0.01$ s (Fig. 8).
- Image processing: phase-shift cartography stored as a (320×240) matrix was filtered using a median filter determined by n , the dimension of the square sub-matrix of filtration. If $n = 1$, there is no filtration, any artifact on a pixel strongly influences the phase contrast, measurement is not reliable, for $n \rightarrow$ infinite, phase contrast tends to 0. A compromise at $n = 9$ appeared satisfactory given the plotted data in Fig. 9.

For a frequency of stimulation $0.1 < f(\text{Hz}) < 1$, more than 40 cumulated periods for demodulation calculation, quasi thermal steady-state and a sub-matrix of filtration with $n \geq 9$, the phase contrast measurement was found reproducible on our component including an experimental noise of 6° systematically observed.

Frequency of stimulation, cumulated periods for demodulation calculation, thermal regime and phase-shift image filtration appeared to be the most sensitive experimental parameters as far as lock-in thermography is concerned. These parameters must

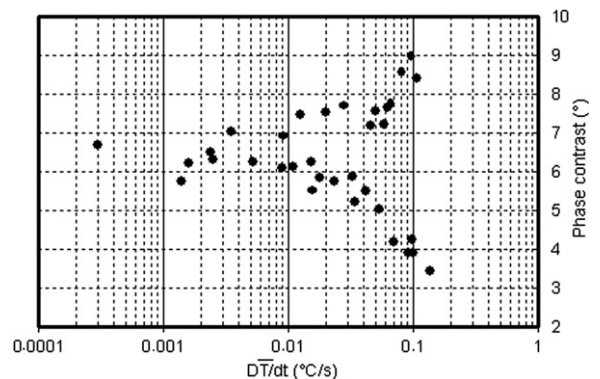


Fig. 8. Phase contrast evaluation vs average temperature gradient (exp. parameters: $f = 0.7$ Hz, >30 periods, $n = 9$).

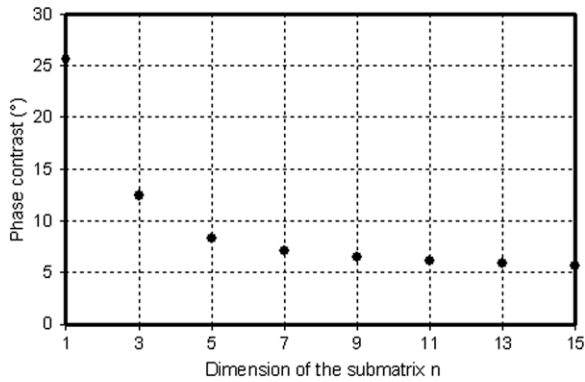


Fig. 9. Phase contrast evaluation vs dimension of the submatrix for median filter (exp. parameters: $f = 0.7$ Hz, >30 periods, quasi steady-state).

be evaluated for each sample geometry for a given test bed.

4. Validation of the experimental protocol

The recorded front surface temperature was compared with 3D modelling. The incident heat flux was imposed as a boundary condition of the calculation and was adjusted step by step to correlate with experimental measurements. A 4 kW/m^2 sinus modulated absorbed heat flux was calculated as shown in Fig. 5.

Afterwards, it was possible to compare numerical results with experimental phase contrast measured on the W7-X PFC with calibrated defects as shown in Fig. 6. Calculations were shifted to take into account the experimental noise of 6° and marked as a line with an uncertainty of $\pm 2^\circ$ on phase shift coming from the $\pm 8\%$ conductivity CFC NB31 scattering. Experimental measurements from cumulated examinations were marked with black spots. Fig. 6 indicates that the minimum size of a detectable strip

defect would be 4 mm at the CFC/copper interface. This detection capability of rather large minimum defect size is however useful for W7-X PFC commissioning.

5. Conclusion

A non destructive technique – so called modulated photothermal thermography or lock-in thermography – has been set-up for CFC armoured plasma facing components (PFC) examination. Reliable measurements of phase contrast were obtained on a 8 mm thick CFC NB31 armoured W7-X divertor component with calibrated defects following a well defined testing protocol and image processing. A 3D finite element analysis allowed the correlation of the measured phase contrast and showed that a 4 mm strip defect could be detected at the CFC/copper interface. Such a fast and easy to operate non destructive technique should be considered in the set of standard examinations for CFC armoured PFC commissioning.

References

- [1] A. Durocher, J. Schlosser, J.J. Cordier, G. Agarici, *Fus. Eng. Des.* 66–68 (2003) 305.
- [2] S. Fouquet, J. Schlosser, M. Merola, A. Durocher, F. Escourbiac, A. Grosman, M. Missirlian, C. Portafaix, *Fus. Eng. Des.* 81 (2006) 265.
- [3] H. Traxler, J. Schlosser, A. Durocher, B. Schedler, T. Huber, A. Zabernig, *Phys. Script T111* (2004) 203.
- [4] D. Wu, A. Salerno, U. Malter, R. Aoki et al., in: *Proc. of QIRT 1996*, Edizioni ETS, Pisa, p. 251.
- [5] P. Appendino, M. Ferraris, V. Casalegno, M. Salvo, M. Merola, M. Grattarola, *J. Nuc. Mater.* 329–333 (2004) 1563.
- [6] J. Boscary, H. Greuner, M. Czerwinski, B. Mendelevitch, K. Pfefferle, H. Renner, *Nucl. Fusion* 43 (2003) 831.
- [7] D. Maillet, S. Andre, J.C. Bastale, A. Degiovanni, Ch. Moyne, *Thermal Quadrupoles: Solving the Heat Equation Through Integral Transforms*, John Wiley, 2000, ISBN 0-471-98320-9.